Joint Tx/Rx Signal Processing for Uplink Distributed Antenna Network using Single-Carrier MU-MIMO

Shinya Kumagai Shohei Yoshioka and Fumiyuki Adachi
Dept. of Communications Engineering, Graduate School of Engineering, Tohoku University
6-6-05, Aza-Aoba, Aramaki, Aoba-ku, Sendai, 980-8579, Japan
{kumagai, yoshioka}@mobile.ecei.tohoku.ac.jp, adachi@ecei.tohoku.ac.jp

Abstract—**A combination of distributed antenna network (DAN), where a number of antennas are spatially distributed within a macro cell, and multi-user (MU) multiple-input multiple-output (MIMO) can achieve high total throughput. Recently, we proposed a minimum mean square error based joint transmit and receive linear filtering (joint Tx/Rx MMSE filtering) for single-carrier (SC)-MU-MIMO uplink. Joint Tx/Rx MMSE filtering transforms the MIMO channel between each user equipment (UE) and base station (BS) to multiple eigenmodes, and applies MMSE based power allocation (PA). MMSE-PA achieves good bit error rate (BER) performance by allocating much power to the eigenmodes having low channel gains (or eigenvalues). However, in DAN, large gaps exist among eigenvalues since the average received signal power of DA is different from each other, and this leads to a significant throughput degradation. Therefore, PA should be designed from the view point of throughput (i.e., Shannon's channel capacity). This paper proposes a joint Tx/Rx WF-MMSE filtering for uplink DAN using SC-MU-MIMO. Water-filling (WF)-PA which maximizes the throughput and MMSE-PA are applied in eigenmode-domain and in frequency-domain, respectively. Numerical results show that proposed filtering achieves better throughput performance than the previously proposed joint Tx/Rx MMSE filtering.**

Keywords-component; distributed antenna; uplink; single-carrier; MU-MIMO; power allocation; UE-DA grouping

I. INTRODUCTION

Distributed antenna network (DAN) [1, 2], where a number of antennas are spatially distributed within a macro cell and connected to base band unit (BBU), is a promising network to improve both the spectral and energy efficiencies of mobile network simultaneously. Therefore, DAN is a good candidate for the fifth generation (5G) mobile network. Furthermore, multi-user multiple-input multiple-output (MU-MIMO) transmission [3], where a base station (BS) communicates with multiple user equipments (UEs) using the same time/frequency, is a powerful technique to increase the total throughput of mobile network. A combination of DAN and MU-MIMO achieves high total throughput since multiple DAs can be visible from multiple UEs with a high probability [4].

Recently, we proposed a minimum mean square error based joint transmit and receive linear filtering (joint Tx/Rx MMSE filtering) for single-carrier (SC)-MU-MIMO uplink, under the assumption that each UE shares the channel state information (CSI) with its associated BS (note that CSI sharing among UEs is not considered) [5]. Broadband SC-MU-MIMO uplink transmission obtains frequency diversity gain while the bit error rate (BER) degrades due to inter-symbol interference (ISI) caused by the channel frequency-selectivity as well as inter-antenna interference (IAI) and inter-user interference (IUI). By applying Tx filtering and Rx filtering to UE and BS, respectively, MIMO channel between each UE and BS is transformed to multiple eigenmodes, to each of which MMSE based Tx power allocation (PA) and Rx frequency-domain equalization (FDE) are applied. Due to the above filtering, IAI and ISI are suppressed significantly. At the same time, IUI is suppressed by BS's Rx filtering. As a consequence, joint Tx/Rx MMSE filtering achieves a better BER performance than the conventional Rx MMSE filtering. Here, MMSE-PA improves the overall BER by allocating much power to the eigenmodes haveing low channel gains (i.e. eigenvalues).

However, in DAN, large gaps exist among eigenvalues since the average received signal power of DA is different from each other. As a consequence, MMSE-PA allocates much power to low eigenmodes, thereby degrading the throughput significantly. Therefore, another PA should be designed. Note that water-filling (WF)-PA [6] enhances ISI when applied to SC transmissions.

This paper studies uplink DAN using SC-MU-MIMO and proposes a joint Tx/Rx WF-MMSE filtering combined with PA. At first, the power is allocated among eigenmodes by the WF-PA. Then, the power allocated to each eigenmode is further allocated among frequencies by the MMSE-PA. As a consequence, ISI is suppressed while avoiding a significant throughput degradation. Numerical results show that proposed joint Tx/Rx WF-MMSE filtering achieves better throughput performance than the previously proposed joint Tx/Rx MMSE filtering.

The remainder of this paper is organized as follows. Sect. II presents the system model. Sect. III presents the signal representation for uplink DAN using SC-MU-MIMO with joint Tx/Rx MMSE filtering, and then derives the PA of joint Tx/Rx WF-MMSE filtering. Sect. IV shows the numerical results, and Sect. V gives the concluding remarks.

Notations: $E[.]$, $[.]^T$, and $[.]^H$ denote the ensemble average operation, the transpose operation, and the Hermitian transpose operation, respectively. $\delta(x)$ and $(x)^+$ denotes the delta function and $\max(0, x)$, respectively. $\mathbf{I}_N$ is the $N\times N$ identity matrix.

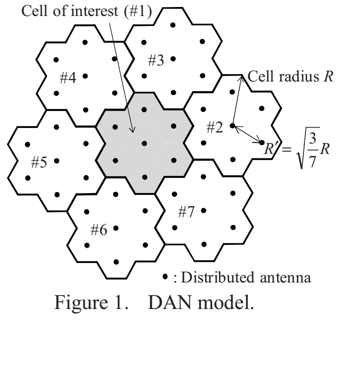

Figure 1. DAN model.

II. SYSTEM MODEL

This section presents the DAN and channel models assumed in this paper, and introduces a dynamic UE-DA grouping to efficiently group the UEs and DAs for MU-MIMO transmissions with low complexity.

A. DAN model

Fig. 1 shows the DAN model [7] assumed in this paper. N_{total}=7 DAs are distributed within each macro cell whose cell radius is denoted as R with the distance $R'=\sqrt{3/7}R$ between each DA. The central cell (#1) is the cell of interest and the 6 surrounding cells (#2~7) are considered. All macro cells are assumed to use the same frequency, and U UEs which have N_{UE} antennas are randomly located within each macro cell.

B. Channel model

The broadband wireless channel is characterized by distance-dependent path loss, log-normally distributed shadowing loss, and multipath fading. Assuming that the channel is composed of L distinct paths, the channel impulse response $h_{m,u,n}^{(c',c)}(\tau)$ between antenna#n of UE#u in macro cell#c and DA#m in macro cell#c' can be represented as

$$h_{m,u,n}^{(c',c)}(\tau) = \left(d_{m,u}^{(c',c)}\right)^{-\frac{\alpha}{2}} \left\{ \begin{array}{l} \sqrt{\dfrac{K}{K+1}} \exp\left(j\theta_{m,u,n}^{(c',c)}\right)\delta\left(\tau-\tau_{m,u,n}^{(c',c)}(1)\right) \\ +\sqrt{10^{-\frac{\eta_{m,u}^{(c',c)}}{10}}} \sqrt{\dfrac{1}{K+1}} \sum_{l=1}^{L} \xi_{m,u,n}^{(c',c)}(l)\delta\left(\tau-\tau_{m,u,n}^{(c',c)}(l)\right) \end{array} \right\}. \quad (1)$$

In this paper, the channel is assumed to be a Nakagami-Rice fading channel (i.e. direct-to-delay path power ratio K>0) when the distance $d_{m,u}^{(c',c)}$ between UE#u in macro cell#c and DA#m in macro cell#c' is equal to or smaller than $R/\sqrt{7}$, and a Rayleigh fading channel (i.e. K=0) when $d_{m,u}^{(c',c)}$ is larger than $R/\sqrt{7}$. α and $\eta_{m,u}^{(c',c)}$ denote the path loss exponent and the shadowing loss in dB having zero-mean and standard deviation σ_S, respectively. $\theta_{m,u,n}^{(c',c)}$ is the phase of direct path and is assumed to be distributed uniformly. $\xi_{m,u,n}^{(c',c)}(l)$ and $\tau_{m,u,n}^{(c',c)}(l)$ are respectively the complex-valued path gain and the time delay of path#l with $E[\sum_{l=1}^{L}\xi_{m,u,n}^{(c',c)}(l)]=1$, $\forall c$, $\forall c'$, $\forall m$, $\forall u$, $\forall n$. In this paper, we assume a symbol-spaced time delay (i.e., $\tau_{m,u,n}^{(c',c)}(l)=l-1$, $\forall c$, $\forall c'$, $\forall m$, $\forall u$, $\forall n$).

The average signal power $P_{r,m,u}^{(c',c)}$ received at DA#m in macro cell#c' for the signal transmitted from UE#u in macro cell#c can be modeled as

$$P_{r,m,u}^{(c',c)} = P_{t,u}^{(c)}\left(d_{m,u}^{(c',c)}\right)^{-\alpha}\left(\frac{K}{K+1}+10^{-\frac{\eta_{m,u}^{(c',c)}}{10}}\frac{1}{K+1}\right), \quad (2)$$

where $P_{t,u}^{(c)}$ is the transmit power of UE#u in macro cell#c and set to $P_{t,u}^{(c)}=P_t$, $\forall c$, $\forall u$ in this paper. By introducing the normalized distance $\hat{d}_{m,u}^{(c',c)}=d_{m,u}^{(c',c)}/R$, the normalized transmit symbol energy $E_s=P_t\cdot R^{-\alpha}\cdot T_s$, and the noise variance $2\sigma^2=2N_0/T_s$, where T_s is the symbol duration and N_0 is the one-sided power spectrum density of additive white Gaussian noise (AWGN), the average received signal-to-noise power ratio (SNR) $\gamma_{m,u}^{(c',c)}$ is expressed as

$$\gamma_{m,u}^{(c',c)} = \frac{P_{r,m,u}^{(c',c)}}{2\sigma^2} = \left(\frac{E_s}{N_0}\right)\left(\hat{d}_{m,u}^{(c',c)}\right)^{-\alpha}\left(\frac{K}{K+1}+10^{-\frac{\eta_{m,u}^{(c',c)}}{10}}\frac{1}{K+1}\right). \quad (3)$$

C. Dynamic UE-DA grouping

The conventional study on DAN [7] assumed that each UE is connected to the DAs within the macro cell where it is located only (called fixed UE-DA grouping in this paper). Therefore, large co-channel interference (CCI) occurred between nearby UEs across cell boundary and the transmission performance degraded significantly. In this subsection, we introduce a dynamic UE-DA grouping, where UEs interfering strongly with each other and the neighboring DAs are grouped over the cell boundary. The dynamic UE-DA grouping can regard strong CCI as IUI and suppress it by MU-MIMO signal processing.

Since UEs and DAs are grouped over the cell boundary, we redefine the UE and DA indexes as u=1~7U and m=1~7N_{total}, respectively. Fig. 2 shows the flowchart of the proposed dynamic UE-DA grouping. Since MU-MIMO transmissions require that the number of DAs be equal to or larger than the total number of multiplexed UE antennas, at first, the DA connected to each UE antenna#n is determined. In this paper, the DA#$a_{u,n}$ which has the highest $\gamma_{m,u}$ (redefined $\gamma_{m,u}^{(c',c)}$ in Eq. (3) by the above indexes) is selected for UE#u's antenna#n as

$$a_{u,n} = \arg\max_{m} \gamma_{m,u} . \quad (4)$$

If DA#$a_{u,n}$ has been already selected as another UE antenna's connected DA, the UE antenna which has lower $\gamma_{m,u}$ is connected to the DA which has the next highest $\gamma_{m,u}$. Note that the DAs except for the 7$N_{UE}U$ selected ones are not used for MU-MIMO transmission in this paper.

After selecting all UE antenna's connected DAs, the initial UE and DA for grouping are determined. At first, the giving interference of UE#u to all DAs except for DA#$a_{u,n}$ connected to UE#u is calculated for all UE#u except for the UEs belonging to the UE set G, which is the universal set of the subset G_g (at the first iteration stage for g, G is the null set). The average giving interference power I_u normalized by the noise power is expressed as

$$I_u = \sum_{i\notin G, i\neq u}\sum_{n=1}^{N_{UE}}\gamma_{a_{i,n},u} . \quad (5)$$

Then, UE#u and the connected DA#$a_{u,n}$ which have the highest I_u are grouped to G_g.

Next, other UEs and DAs which are grouped to G_g are determined. At first, the summation of receiving interference of DA#$a_{u,n}$ connected to UE#u from the UEs in group G_g and giving interference of UE#u to DAs in group G_g is calculated for all UE#u except for the UEs in group G. The average mutual interference power J_u normalized by the noise power is expressed as

$$J_u = \sum_{i\in G_g}\sum_{n=1}^{N_{UE}}\gamma_{a_{u,n},i} + \sum_{i\in G_g}\sum_{n=1}^{N_{UE}}\gamma_{a_{i,n},u} . \quad (6)$$

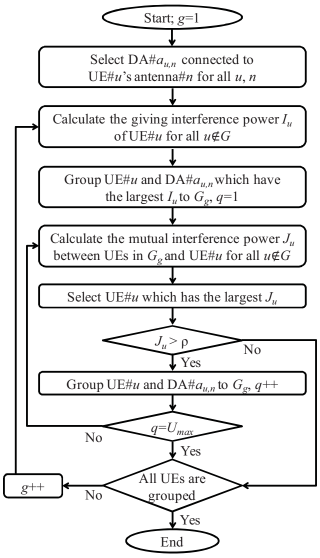

Figure 2. Flowchart of dynamic UE-DA grouping.

Then, UE#u which has the highest J_u is selected, and if the J_u is equal to or higher than threshold ρ, UE#u and the connected DA#$a_{u,n}$ are grouped to G_g. The above grouping steps to G_g are repeated until the maximum J_u is lower than threshold ρ or the number of belonging UEs to G_g is equal to the maximum number U_{max} of UEs, and then, group G_g is fixed.

After fixing group G_g, the grouping goes back to the calculation of I_u for group G_{g+1}, and repeats the grouping steps until all UEs are grouped to G.

III. SC-MU-MIMO Uplink Transmission

In this section, without loss of generality, the signal representations for group G_g which is determined by the dynamic UE-DA grouping shown in Sect. II-C is given. Fig. 3 shows the system model of SC-MU-MIMO uplink assumed in this paper. U_g UEs which have N_{UE} antennas communicate with $N_{UE}U_g$ DAs. It is assumed that each UE knows the CSI between itself and $N_{UE}U_g$ DAs only (i.e., CSI sharing among UEs is not considered). At first, the signal representations for joint Tx/Rx MMSE filtering proposed in [5] is presented, and then, the PA for joint Tx/Rx WF-MMSE filtering proposed in this paper is derived.

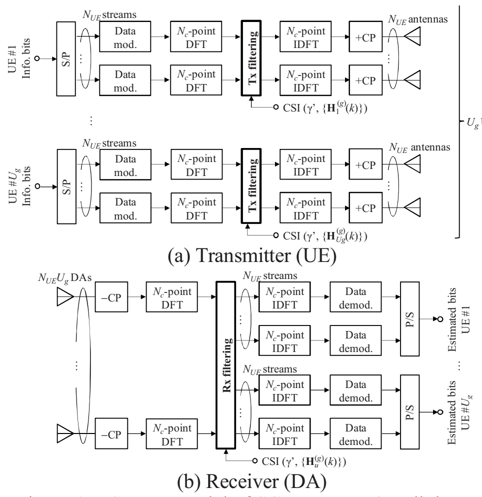

Figure 3. System model of SC-MU-MIMO uplink.

A. Tx/Rx signal representations

The channel transfer function $H^{(g,g')}_{m,u,n}(k)$ between UE#u's antenna#n in group $G_{g'}$ and DA#m in group at the k(=1~N_c)-th frequency is given by

$$H^{(g,g')}_{m,u,n}(k)=\left(\hat{d}^{(g,g')}_{m,u}\right)^{-\frac{\alpha}{2}}\times\left\{\begin{array}{l}\sqrt{\dfrac{K}{K+1}}\exp\left(j\theta^{(g,g')}_{m,u,n}\right)\exp\left(-j\dfrac{2\pi k\tau^{(g,g')}_{m,u,n}(1)}{N_c}\right)\\+\sqrt{10^{-\frac{\eta^{(g,g')}_{m,u}}{10}}}\sqrt{\dfrac{1}{K+1}}\sum_{l=1}^{L}\xi^{(g,g')}_{m,u,n}\exp\left(-j\dfrac{2\pi k\tau^{(g,g')}_{m,u,n}(l)}{N_c}\right)\end{array}\right\},\quad(7)$$

where N_c is the block size, and the value of each variable is corresponding to that in Eq. (1). Since the CCI power received at each DA is different from each other in DAN, a normalization is introduced to use the same signal representations as [5]. Assuming CCI can be approximated as a complex-valued random variable, the variance of noise + CCI at DA#m is expressed as

$$\begin{aligned}2\left(\sigma^{(g)}_{\text{noise+CCI},m}\right)^2&=\frac{2N_0}{T_s}+\frac{2E_s}{T_s}\frac{1}{N_c}\sum_{g'\neq g}\sum_{u\in G_{g'}}\sum_{n=1}^{N_{UE}}\sum_{k=1}^{N_c}\left|H^{(g,g')}_{m,u,n}(k)\right|^2\\&=\frac{2N_0}{T_s}\left(1+\frac{\gamma'}{N_c}\sum_{g'\neq g}\sum_{u\in G_{g'}}\sum_{n=1}^{N_{UE}}\sum_{k=1}^{N_c}\left|H^{(g,g')}_{m,u,n}(k)\right|^2\right)\\&\equiv\frac{2N_0}{T_s}\left(1+\beta^{(g)}_m\right),\end{aligned}\quad(8)$$

where $\gamma'=E_s/N_0$. By defining the (m,n)-th component of the channel matrix $\mathbf{H}^{(g)}_u(k)\in\mathbb{C}^{N_{UE}N_g\times N_{UE}}$ between UE#u and DAs in G_g as $H^{(g,g)}_{m,u,n}(k)\big/\sqrt{\beta^{(g)}_m}$, the variance of equivalent noise (noise + CCI) is given by $2N_0/T_s$.

At UE#u, information bit sequence is serial-to-parallel (S/P) converted to N_{UE} parallel bit sequences, and then each sequence is data-modulated. Each data symbol sequence is divided to N_c-symbol blocks and each symbol block is transformed into a frequency-domain symbol block by N_c-point discrete Fourier transform (DFT). The Tx symbol vector $\mathbf{S}^{(g)}_u(k)\in\mathbb{C}^{N_{UE}\times 1}$ at the k-th frequency is obtained by applying the Tx filtering to the frequency-domain data symbol vector $\mathbf{D}^{(g)}_u(k)\in\mathbb{C}^{N_{UE}\times 1}$ at the k-th frequency, which is expressed as

$$\mathbf{S}^{(g)}_u(k)=[S^{(g)}_{u,1}(k)\cdots S^{(g)}_{u,N_{UE}}(k)]^T=\sqrt{\frac{2E_s}{T_s}}\mathbf{W}^{(g)}_{t,u}(k)\mathbf{D}^{(g)}_u(k),\quad(9)$$

where $\mathbf{W}^{(g)}_{t,u}(k)\in\mathbb{C}^{N_{UE}\times N_{UE}}$ is the Tx filter matrix, and the MMSE-based filter is expressed as

$$\mathbf{W}^{(g)}_{t,u}(k)=\mathbf{V}^{(g)}_u(k)\sqrt{\mathbf{\Phi}^{(g)}_{\text{MMSE},u}(k)}\,,\quad(10)$$

with $\mathbf{V}^{(g)}_u(k)\in\mathbb{C}^{N_{UE}\times N_{UE}}$ being the unitary matrix whose each column has the right singular vector of $\mathbf{H}^{(g)}_u(k)$. The n-th diagonal component $\Phi^{(g)}_{\text{MMSE},u,n}(k)$ of the diagonal matrix $\mathbf{\Phi}^{(g)}_{\text{MMSE},u}(k)\in\mathbb{R}^{N_{UE}\times N_{UE}}$ is the MMSE-based transmit PA to the n-th eigenmode at the k-th frequency (whose eigenvalue $\Lambda^{(g)}_{u,n}(k)$), and is expressed as

$$\Phi^{(g)}_{\mathrm{MMSE},u,n}(k)=\left(\frac{1}{\sqrt{\nu^{(g)}_u}}\frac{1}{\sqrt{\gamma'\Lambda^{(g)}_{u,n}(k)}}-\frac{1}{\gamma'\Lambda^{(g)}_{u,n}(k)}\right)^+, \quad (11)$$

where $\nu^{(g)}_u$ is chosen to satisfy the per-UE Tx power constraint (i.e. $\sum_{k=1}^{N_c}\sum_{n=1}^{N_{UE}}\Phi^{(g)}_{\mathrm{MMSE},u,n}(k)=N_{UE}N_c$). N_c-point inverse DFT (IDFT) is applied to each Tx symbol block { $S^{(g)}_{u,n}(k)$; k=1~N_c}, n=1~N_{UE}, to transform back to time-domain Tx blocks. Finally, the last N_g symbols of each Tx block are copied as a cyclic prefix (CP) and inserted into the guard interval (GI) at the beginning of each Tx block and then transmitted from N_{UE} antennas.

At the receiver, each CP is removed from the signal blocks received by $N_{UE}N_g$ antennas and then, each block is transformed into the frequency-domain Rx signal block by N_c-point DFT. The frequency-domain received signal vector $\mathbf{R}^{(g)}(k)\in\mathbb{C}^{N_{UE}N_g\times 1}$ at the k-th frequency after N_c-point DFT is expressed as

$$\begin{aligned}&\mathbf{R}^{(g)}(k)\\&=\sqrt{\frac{2E_s}{T_s}}\left[\mathbf{H}^{(g)}_1(k)\mathbf{W}^{(g)}_{t,1}(k)\cdots\mathbf{H}^{(g)}_{U_g}(k)\mathbf{W}^{(g)}_{t,U_g}(k)\right]\begin{bmatrix}\mathbf{D}^{(g)}_1(k)\\ \vdots\\ \mathbf{D}^{(g)}_{U_g}(k)\end{bmatrix}+\mathbf{Z}^{(g)}(k)\\&\equiv\sqrt{\frac{2E_s}{T_s}}\overline{\mathbf{H}}^{(g)}(k)\overline{\mathbf{D}}^{(g)}(k)+\mathbf{Z}^{(g)}(k),\end{aligned} \quad (12)$$

where $\mathbf{Z}^{(g)}(k)\in\mathbb{C}^{N_{UE}N_g\times 1}$ is the noise + CCI vector whose elements are zero-mean complex-valued random variables having variance $2N_0/T_s$. The frequency-domain soft-output symbol vector $\hat{\mathbf{D}}^{(g)}(k)\in\mathbb{C}^{N_{UE}N_g\times 1}$ is obtained by applying the Rx filtering on $\mathbf{R}^{(g)}(k)$ as

$$\begin{aligned}\hat{\mathbf{D}}^{(g)}(k)&=[\hat{D}^{(g)}_1(k)\cdots\hat{D}^{(g)}_{N_{UE}U_g}(k)]^T\\&=\mathbf{W}^{(g)}_r(k)\mathbf{R}^{(g)}(k)\\&=\sqrt{\frac{2E_s}{T_s}}\mathbf{W}^{(g)}_r(k)\overline{\mathbf{H}}^{(g)}(k)\overline{\mathbf{D}}^{(g)}(k)+\mathbf{W}^{(g)}_r(k)\mathbf{Z}^{(g)}(k),\end{aligned} \quad (13)$$

where $\mathbf{W}^{(g)}_r(k)\in\mathbb{C}^{N_{UE}U_g\times N_{UE}U_g}$ is the Rx filter matrix, and the MMSE-based filter is expressed as

$$\begin{aligned}\mathbf{W}^{(g)}_r(k)&=\left[\left(\mathbf{W}^{(g)}_{r,1}(k)\right)^T\ldots\left(\mathbf{W}^{(g)}_{r,U_g}(k)\right)^T\right]^T\\&=\left\{\left(\overline{\mathbf{H}}^{(g)}(k)\right)^H\overline{\mathbf{H}}^{(g)}(k)+\gamma'^{-1}\mathbf{I}_{N_{UE}U_g}\right\}^{-1}\left(\overline{\mathbf{H}}^{(g)}(k)\right)^H.\end{aligned} \quad (14)$$

N_c-point IDFT is applied to each frequency-domain soft-output symbol block { $\hat{D}^{(g)}_m(k)$; k=1~N_c}, m=1~$N_{UE}U_g$ and then, the time-domain soft-output symbol blocks are obtained.

Based on Shannon's channel capacity, the throughput $C^{(g)}_u$ (bps/Hz) of UE#u using the above joint Tx/Rx MMSE filtering is expressed as

$$C^{(g)}_u=\sum_{n=1}^{N_{UE}}\log_2\left(1+\Gamma^{(g)}_{u,n}\right), \quad (15)$$

where $\Gamma^{(g)}_{u,n}$ is the received signal-to-interference plus noise power ratio (SINR) of UE#u's n-th eigenmode after joint Tx/Rx MMSE filtering expressed as

$$\Gamma^{(g)}_{u,n}=\left|\widetilde{H}^{(g)}_{u,n}\right|^2\Big/\left(\mu^{(g)}_{\mathrm{ISI},u,n}+\mu^{(g)}_{\mathrm{IAI},u,n}+\mu^{(g)}_{\mathrm{IUI},u,n}+\mu^{(g)}_{\mathrm{noise+CCI},u,n}\right), \quad (16)$$

$$\begin{cases}\widetilde{H}^{(g)}_{u,n}=\dfrac{1}{N_c}\displaystyle\sum_{k=1}^{N_c}\hat{H}^{(g)}_{u,n,n}(k)\\ \hat{H}^{(g)}_{u,n,n''}(k)=\displaystyle\sum_{m=1}^{N_{UE}U_g}W^{(g)}_{r,u,n,m}(k)\sum_{n'=1}^{N_{UE}}H^{(g)}_{u,m,n'}(k)W^{(g)}_{t,u,n',n''}(k)\\ \mu^{(g)}_{\mathrm{ISI},u,n}=\dfrac{1}{N_c}\displaystyle\sum_{k=1}^{N_c}\left|\hat{H}^{(g)}_{u,n,n}(k)\right|^2-\left|\widetilde{H}^{(g)}_{u,n}\right|^2\\ \mu^{(g)}_{\mathrm{IAI},u,n}=\dfrac{1}{N_c}\displaystyle\sum_{\substack{n''=1\\n''\neq n}}^{N_{UE}}\sum_{k=1}^{N_c}\left|\hat{H}^{(g)}_{u,n,n''}(k)\right|^2\\ \mu^{(g)}_{\mathrm{IUI},u,n}=\dfrac{1}{N_c}\displaystyle\sum_{\substack{u'=1\\u'\neq u}}^{U_g}\sum_{n''=1}^{N_{UE}}\sum_{k=1}^{N_c}\left|\sum_{m=1}^{N_{UE}U_g}\begin{pmatrix}W^{(g)}_{r,u,n,m}(k)\\ \times\displaystyle\sum_{n'=1}^{N_{UE}}H^{(g)}_{u',m,n'}(k)W^{(g)}_{t,u',n',n''}(k)\end{pmatrix}\right|^2\\ \mu^{(g)}_{\mathrm{noise+CCI},u,n}=\dfrac{\gamma'^{-1}}{N_c}\displaystyle\sum_{m=1}^{N_{UE}U_g}\sum_{k=1}^{N_c}\left|W^{(g)}_{r,u,n,m}(k)\right|^2\end{cases} \quad (17)$$

$W^{(g)}_{r,u,n,m}(k)$, $H^{(g)}_{u,m,n'}(k)$, and $W^{(g)}_{t,u,n,n'}(k)$ are the (n,m)-th, (m,n)-th, and (n,n')-th components of $\mathbf{W}^{(g)}_{r,u}(k)$, $\mathbf{H}^{(g)}_u(k)$, and $\mathbf{W}^{(g)}_{t,u}(k)$, respectively. $\mu^{(g)}_{\mathrm{ISI},u,n}$, $\mu^{(g)}_{\mathrm{IAI},u,n}$, $\mu^{(g)}_{\mathrm{IUI},u,n}$, and $\mu^{(g)}_{\mathrm{noise+CCI},u,n}$ are the variances of normalized residual ISI, IAI, IUI, and noise + CCI, respectively.

B. Derivation of new power allocation

The MMSE-PA given by Eq. (11) minimizes the overall MSE by allocating much power to the eigenmodes which have low eigenvalues, and degrades the throughput significantly. On the other hand, WF-PA among eingemodes and frequencies enhances ISI. Furthermore, it is difficult to derive the PA which maximizes Eq. (15) in closed-form. Therefore, in this paper at first, we define a virtual throughput using the frequency-average of eigenvalues, and derive the eigenmode-domain PA which maximizes the virtual throughput. Next, we derive the frequency-domain PA which further allocates the Tx power allocated to each eigenmode by the above PA based on MMSE criterion.

The virtual throughput $\overline{C}^{(g)}_u$ (bps/Hz) is defined using the frequency-average $\overline{\Lambda}^{(g)}_{u,n}=\sum_{k=1}^{N_c}\Lambda^{(g)}_{u,n}(k)/N_c$ of eigenvalues of UE#u's n-th eigenmode as

$$\overline{C}^{(g)}_u\equiv\sum_{n=1}^{N_{UE}}\log_2\left(1+\gamma'\Omega^{(g)}_{\mathrm{WF},u,n}\overline{\Lambda}^{(g)}_{u,n}\right), \quad (18)$$

where $\Omega^{(g)}_{\mathrm{WF},u,n}$ is the PA to the n-th eigenmode, and $\Omega^{(g)}_{\mathrm{WF},u,n}$ which maximizes Eq. (18) is expressed as (the derivation is omitted)

$$\Omega^{(g)}_{\mathrm{WF},u,n}=\left(\frac{1}{\kappa^{(g)}_u}-\frac{1}{\gamma'\overline{\Lambda}^{(g)}_{u,n}}\right)^+, \quad (19)$$

with $\kappa_u^{(g)}$ being chosen to satisfy the per-UE Tx power constraint (i.e. $\sum_{n=1}^{N_{UE}} \Omega_{\mathrm{WF},u,n}^{(g)} = N_{UE} N_c$).

Next, as [5], assuming IAI and IUI are perfectly removed at the receiver, the virtual MSE $\varepsilon_{u,n}^{(g)}$ of UE#u's n-th eigenmode is defined as

$$\varepsilon_{u,n}^{(g)} \equiv \sum_{k=1}^{N_c} \left(\gamma'^{-1} \Lambda_{u,n}^{(g)}(k) \Psi_{\mathrm{MMSE},u,n}^{(g)}(k) + 1 \right)^{-1}, \qquad (20)$$

where $\Psi_{\mathrm{MMSE},u,n}^{(g)}(k)$ is the PA to the k-th frequency on the n-th eigenmode, and $\Psi_{\mathrm{MMSE},u,n}^{(g)}(k)$ which minimizes Eq. (20) is expressed as (the derivation is omitted)

$$\Psi_{\mathrm{MMSE},u,n}^{(g)}(k) = \left(\frac{1}{\sqrt{\lambda_{u,n}^{(g)}}} \frac{1}{\sqrt{\gamma' \Lambda_{u,n}^{(g)}(k)}} - \frac{1}{\gamma' \Lambda_{u,n}^{(g)}(k)} \right)^{+}, \qquad (21)$$

with $\lambda_{u,n}^{(g)}$ being chosen to satisfy the per-eignmode allocated power constraint (i.e. $\sum_{k=1}^{N_c} \Psi_{\mathrm{MMSE},u,n}^{(g)}(k) = \Omega_{\mathrm{WF},u,n}^{(g)}$).

In this paper, we call the joint Tx/Rx filtering which applies the PA given by Eqs. (19) and (21) as joint Tx/Rx WF-MMSE filtering.

IV. NUMERICAL RESULTS

In the numerical evaluation, U=2 UEs having N_{UE}=2 antennas are located in each macro cell and E_s/N_0=10(dB). The size N_c=128 of DFT/IDFT and the GI length N_c=16. The channel is assumed to have the path loss exponent α=3.5, shadowing loss standard deviation σ_S=7(dB), and a 16-path uniform power delay profile. K=10(dB) in Nakagami-Rice environment. Uncorrelated fading among paths/antennas/UEs is assumed. Each UE knows the perfect CSI between itself and DAs, and SPC knows the perfect CSI between all UEs and DAs. The threshold ρ=0 in the dynamic UE-DA grouping (i.e., U_{max} UEs belong to the same group inevitably).

Fig. 4 plots the throughput distribution of uplink DAN using SC-MU-MIMO with proposed joint Tx/Rx WF-MMSE filtering for several values of U_{max} in dynamic UE-DA grouping, where x% outage throughput is defined as that which the total UE throughput in the cell of interest falls below with probability of x%. The performance with joint Tx/Rx MMSE filtering proposed in [5] and conventional Rx MMSE filtering are also plotted for comparison. The performance when DAs only within the same macro cell cooperate (fixed UE-DA grouping) is also plotted.

Fig. 4 shows that the proposed joint Tx/Rx WF-MMSE filtering achieves higher throughput than both joint Tx/Rx MMSE filtering and Rx MMSE filtering. This is because the eigenmode transmission suppresses IAI, and WF and MMSE PAs suppress ISI while avoiding a significant throughput degradation. Fig. 4 also shows that throughput is improved by increasing U_{max} when the dynamic UE-DA grouping is used. When U_{max}=2, slight throughput improvement is obtained since the maximum multiplexing order ($N_{UE}U_g$) in each group is 4, which is the same as the fixed UE-DA grouping ($N_{UE}U$). However, when U_{max}>2, large throughput improvement is obtained since the maximum multiplexing order in each group is larger than 4.

V. CONCLUSION

This paper proposed a joint Tx/Rx WF-MMSE filtering combined with PA for uplink DAN using SC-MU-MIMO. ISI, IAI, and IUI are sufficiently suppressed while avoiding a significant throughput degradation. Numerical results showed proposed joint Tx/Rx WF-MMSE filtering achieves higher throughput than the conventional joint Tx/Rx MMSE filtering.

ACKNOWLEDGMENT

This research was funded by the national project "Research and Development on 5G mobile communications system", supported by the Ministry of Internal Affairs and Communications (MIC), Japan.

REFERENCES

[1] F. Adachi, K. Takeda, T. Yamamoto, R. Matsukawa, and S. Kumagai, "Recent advances in single-carrier distributed antenna network," *Wirel. Commun. Mob. Comput.*, vol. 11, no. 12, pp. 1551-1563, Dec. 2011.

[2] W. Choi and J. G. Andrews, "Downlink performance and capacity of distributed antenna systems in a multicell environment," *IEEE Trans. Wirel. Commun.*, vol. 6, no. 1, pp. 69-73, Apr. 2007.

[3] D. Gesbert, M. Kountouris, R. W. Heath Jr., C.-B. Chae, and T. Sälzer, "Shifting the MIMO paradigm," *IEEE Signal Process. Mag.*, vol. 24, no. 5, pp. 36-46, Oct. 2007.

[4] R. Heath, S. Peters, Y. Wang, and J. Zhang, "A current perspective on distributed antenna systems for the downlink of cellular systems," *IEEE Commun. Mag.*, vol. 51, no. 4, pp. 161-167, Apr. 2013.

[5] S. Kumagai and F. Adachi, "Joint Tx/Rx MMSE filtering for single-carrier MU-MIMO uplink," *12th IEEE Asia Pacific Wireless Communications Symposium (APWCS 2015)*, Singapore, Aug. 2015.

[6] D. Tse and P. Viswanath, *Fundamentals of wireless communication*, Cambridge University Press, 2005.

[7] S. Inoshita, H. Miyazaki, and F. Adachi, "Complexity- reduced per-antenna multiple access interference cancellation for DAN using DS-CDMA," *in Proc. of IEEE 80th Vehicular Technology Conference (VTC2014-Fall)*, Vancouver, Canada, Sep. 2014.

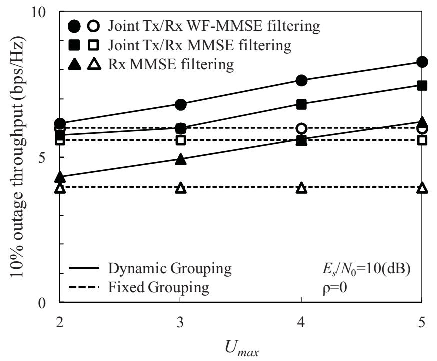

(a) 10% outage throughput

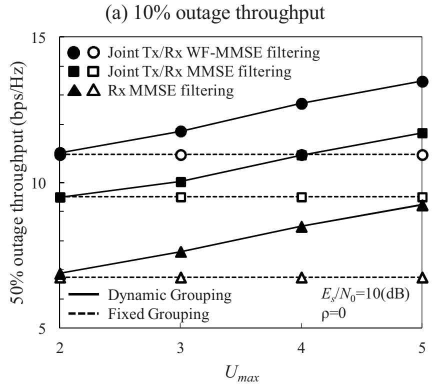

(b) 50% outage throughput

Figure 4. Throughput distribution.